International Journal of Pharmaceutics 373 (2009) 55–61

Contents lists available at ScienceDirect

International Journal of Pharmaceutics

journal homepage: www.elsevier.com/locate/ijpharm

Theoretical investigation of passive intestinal membrane permeability using Monte Carlo method to generate drug-like molecule population

Kiyohiko Sugano*

Global Research & Development, Sandwich Laboratories, Research Formulation, Pfizer Inc., CT13 9NJ Sandwich, Kent, UK

ARTICLE INFO

Article history:
Received 5 November 2008
Received in revised form 30 January 2009
Accepted 3 February 2009
Available online 12 February 2009

Keywords:
Permeability
Simulation
Drug like
Oral absorption
Paracellular
Transcellular
Unstirred water layer

ABSTRACT

The purpose of the present study was to investigate the effect of the physiological and morphological differences between in vivo and in vitro systems on the estimation of in vivo effective intestinal membrane permeability (P_{eff}) from in vitro permeability data ($P_{ivt,app}$). Five hundred virtual drug-like compounds were generated using Monte Carlo method based on the distribution of octanol water partition coefficient, molecular weight, and pK_a. In vivo and in vitro membrane permeability was theoretically calculated from these parameters considering the transcellular, paracellular and unstirred water layer (UWL) permeation. More than 50% of drug-like compounds showed high P_{eff} values. When the same pH value was used for in vivo and in vitro, the scattering of the $P_{ivt,app}$–P_{eff} plot was small, whereas it was large when different pH values were used. However, the extent of discrepancy depended on the physicochemical properties and permeation characteristics of a drug. When the pH effect was directly corrected on the P_{eff} value, paracellular and UWL permeability was inappropriately corrected since the pH partition theory is only applicable for transcellular permeation. In vivo species differences of P_{eff} and the fraction of a dose absorbed (Fa%) was also investigated for humans, rats and dogs. In conclusion, P_{eff} estimation from in vitro data should be based on the theoretical method rather than simple linear regression.

1. Introduction

Oral absorption simulation is one of the key techniques used to improve the efficacy of drug discovery and development (van de Waterbeemd and Gifford, 2003). For accurate simulation, accurate estimation of in vivo effective small intestinal membrane permeability (P_{eff}) is required. An apparent in vitro membrane permeability value ($P_{ivt,app}$), such as Caco-2 permeability, was often used to estimate P_{eff} by simple empirical linear regression (Parrott and Lave, 2008). However, the effect of physiological and morphological differences between the in vivo and in vitro membranes would be non-linear.

The passive membrane permeability consists of transcellular and paracellular pathways. The unstirred water layer (UWL) which is adjacent to the membrane also affects the permeability. The following differences between in vivo intestinal membrane and in vitro cellular membrane would have large effects on P_{eff} estimation: (1) thickness of the unstirred water layer, (2) pH at the membrane surface, (3) pore radius and electric charge of paracellular pathway, and (4) morphological differences, i.e., villi and folds structure.

The thickness of the UWL largely differs between in vivo and in vitro. In vivo, the mucus layer maintains the UWL from effective agitation in the GI lumenal fluid. The mucus layer thickness was reported to be 100–300 μm (Atuma et al., 2001; Fagerholm and Lennernaes, 1995). However, in vitro UWL thickness can be 1500–4000 μm due to the ineffective agitation in well plates (Youdim et al., 2003).

The microclimate pH differs depending on GI position, i.e., pH 5.5–6.7 in the small intestine (Said et al., 1986; Yamashita et al., 2000). Therefore, it would be appropriate to use several pH conditions for in vitro experiments to estimate P_{eff} at different GI positions. However, considering the resource requirement for an in vitro cellular assay, one or two pH conditions are usually used in drug discovery. In addition, for the efflux ratio estimation, pH 7.4 is usually used for both apical and basolateral sides (Shirasaka et al., 2008).

The pore radius of the paracellular pathway also differs among in vivo and in vitro systems. Dogs have a larger pore radius than humans and rats (He et al., 1998). The pore radius of an in vitro membrane differs depending on the cellular system and culture conditions. The pore radius of the Caco-2 membrane tends to be smaller than that of the human small intestine (Knipp et al., 1997), whereas the pore radius of a rat intestinal cell line 2/4/A1 is similar to that of the human small intestine (Tavelin et al., 2003).

* Tel.: +44 1304 644338.
E-mail address: Kiyohiko.Sugano@pfizer.com.

0378-5173/$ – see front matter © 2009 Elsevier B.V. All rights reserved.
doi:10.1016/j.ijpharm.2009.02.002

The morphology of the in vivo small intestinal membrane is different from that of the in vitro membrane. The intestinal membrane has a folds and villi structure which expands the surface area for drug absorption, whereas the in vitro cellular membrane is planar. The morphological difference is the main reason for one or two order differences in the permeability value. The effect of the morphological differences on permeability is non-linear and depends on the permeation characteristics (Oliver et al., 1998; Winne, 1978).

The purpose of the present study was to investigate the effect of physiological and morphological differences on the estimation of P_{eff} from $P_{ivt,app}$. Previously, a theoretical scheme to calculate P_{eff} from intrinsic transcellular permeability, pK_a and molecular weight was reported (Obata et al., 2005; Sugano et al., 2003, 2006, 2002). In these reports, the parallel artificial membrane permeability assay (PAMPA) and the octanol water partition coefficient ($\log P_{oct}$) were used as surrogates of intrinsic transcellular permeability. In the present study, the Monte Carlo method was used to generate virtual compounds with drug-like physicochemical properties, and P_{eff} and $P_{ivt,app}$ were calculated from these physicochemical properties to investigate the relationship between P_{eff} and $P_{ivt,app}$.

2. Theory

The main frame of the theoretical estimation of P_{eff}, $P_{ivt,app}$ and the fraction of a dose absorbed (Fa%) from the physicochemical properties of a drug is firstly described, followed by the sub frames.

2.1. Main frame of theoretical estimation of P_{eff}, $P_{ivt,app}$ and Fa% from physicochemical properties

(1) Calculate passive transcellular membrane permeability ($P_{ivx,trans}$, the subscript ivx indicates in vivo or in vitro) from intrinsic passive transcellular membrane permeability ($P_{ivx,trans,0}$, permeability of undissociated species) by multiplying the fraction of undissociated species (f_0) at the pH of in vitro assay or in vivo microclimate pH.

$$P_{ivx,trans} = f_0 \times P_{ivx,trans,0} \quad (1)$$

(2) Add paracellular pathway permeability ($P_{ivx,para}$) to $P_{ivx,trans}$ to give total passive membrane permeability ($P_{ivx,m,tot}$).

$$P_{ivx,m,tot} = P_{ivx,trans} + P_{ivx,para} \quad (2)$$

(3) (only for in vivo) Multiply $P_{ivv,m,tot}$ by the villi surface accessibility (Acc) and maximum villi expansion (VE) to give $P'_{ivv,m,tot}$.

$$P'_{ivv,m,tot} = \mathrm{Acc} \times \mathrm{VE} \times P_{ivv,m,tot} \quad (3)$$

For humans and dogs, VE = ca. 10 (Oliver et al., 1998), whereas 3.5–7.8 for rats (5 was used in this study) (DeSesso and Williams, 2008; Masaoka et al., 2006).

(4) Calculate the membrane permeability across villi surface (P_{villi}) or apparent in vitro membrane permeability value ($P_{ivt,app}$) by adding unstirred water layer permeability (P_{ivxUWL}).

$$P^{-1}_{ivt,app} = P^{-1}_{ivt,app} + P^{-1}_{ivtUWL} \quad (4)$$

$$P^{-1}_{villi} = P'^{-1}_{ivx,m,tot} + P^{-1}_{ivvUWL} \quad (5)$$

(5) (only for in vivo) Calculate P_{eff} by multiplying P_{villi} by the fold expansion (FE). FE differs depending on the in vivo species and GI position. For humans, FE = ca. 3, whereas FE = ca. 1 for rats and dogs (DeSesso and Jacobson, 2001; DeSesso and Williams, 2008).

$$P_{eff} = P_{villi} \times \mathrm{FE} \quad (6)$$

(6) Calculate absorption rate constant (k_a) and Fa% from P_{eff} as

$$k_a = \frac{2}{r_{GI}} \times \mathrm{DF} \times P_{eff} \quad (7)$$

where r_{GI} is the radius of GI tract (1.5 cm for humans, 0.5 cm for dogs and 0.2 cm for rats) (DeSesso and Jacobson, 2001; DeSesso and Williams, 2008; Kararli, 1995; Sutton, 2004) and DF is the degree of flatness of the intestinal tube (Chiou, 1994). DF was previously estimated to be 1.7 from the Fa%–P_{eff} relationship (Sugano, 2008) and the same value was used for rats, dogs and humans. Fa% was calculated as,

$$\mathrm{Fa\%} = (1 - \exp(-k_a \times T_{si})) \times 100 \quad (8)$$

where T_{si} is the small intestinal transit time (3.5 h for humans, 2 h for dogs and rats) (DeSesso and Jacobson, 2001; DeSesso and Williams, 2008; Kararli, 1995; Masaoka et al., 2006; Sutton, 2004).

2.2. Sub frames

2.2.1. Calculation of intrinsic transcellular permeability

$P_{ivx,trans}$ was calculated based on the octanol water partition coefficient.

$$P_{ivv,trans,0} = A \times P^B_{ivt,trans,0} = 2.36 \times 10^{-6} P^{1.1}_{oct} \quad (9)$$

In this study, the intrinsic transcellular permeability was assumed to be same for in vitro and in vivo. Therefore, $A = B = 1$. The coefficient of 2.36×10^{-6} and the power of 1.1 were obtained from the relationship between P_{oct} and $P_{ivt,trans,0}$ (Avdeef et al., 2005b).

2.2.2. Fraction of unionized species

The Henderson-Hasselbalch equation was used for f_0 calculation.

$$f_0 = \frac{1}{1 + ([H^+]/[K_a])} \quad \text{for basic compound} \quad (10)$$

$$f_0 = \frac{1}{1 + ([K_a]/[H^+])} \quad \text{for acidic compound} \quad (11)$$

2.2.3. Calculation of paracellular pathway permeability

Paracellular pathway permeation can be modelled as the permeation through an aqueous cylinder.

$$P_{para} = 3.9 \times 10^{-4} \cdot \frac{1}{\mathrm{MW}^{1/3}} \cdot \mathrm{RK}\left(\frac{\mathrm{MW}^{1/3}}{R_{para,MW}}\right) \times \left(f_0 + \sum^{z(z\neq 0)} f_z \cdot E(z)\right) \quad (12)$$

$$RK(R_{ratio}) = (1 - R_{ratio})^2 (1 - 2.104 \cdot R_{ratio} + 2.09(R_{ratio})^3 - 0.95(R_{ratio})^5) \quad (13)$$

$$E(z) = \frac{C \cdot z}{1 - \exp(-C \cdot z)} \quad (14)$$

where MW is the molecular weight, $R_{para,MW}$ is the paracellular radius based on the cube root of molecular weight (8.6 for humans and rats, 12.9 for dogs, and 5 for the in vitro cellular membrane (assumes Caco-2)), $R_{ratio} = \mathrm{MW}^{1/3}/R_{para,MW}$, C is the electric charge factor of paracellular pathway (2.4 for humans, rats and dogs, and 1.7 for in vitro (assumes Caco-2)), z is the charge of molecular species, and f_z is the fraction of the charge species. The coefficient of 3.9×10^{-4} in Eq. (12) was obtained from the previously reported value for P_{eff} calculation (0.0241) (Sugano et al., 2002)

Table 1
Observed and theoretically predicted P_{eff} and Fa%.

Compound[a]	MW	pK_a[b,c]	log P_{oct}[b]	Observed data						Predicted data					
				P_{eff}			Fa%			P_{eff}			Fa%		
				Human[d]	Dog[e]	Rat[f]	Human[a]	Dog[g]	Rat[h]	Human	Dog	Rat	Human	Dog	Rat
Amiloride	230	8.65 (B)	−1.03[a]	−3.8	–	–	50	–	–	−4.5	−4.2	−5.3	60	95	49
Antipyrine	188	–	0.56	−3.3	–	−4.2	97	–	100	−3.7	−4.1	−4.4	100	98	99
Atenolol	266	9.54 (B)	0.22	−4.7	–	−4.8	50	100	49	−4.6	−4.3	−5.4	48	91	38
Carbamazepine	236	–	2.45	−3.4	–	−4.2	–	–	–	−3.1	−3.6	−3.6	100	100	100
Cimetidine	241	6.93 (B)	0.48	−4.6	–	−4.3	64	98	100	−4.1	−4.2	−4.9	89	95	80
Creatinine	113	–	−1.82[a]	−4.5	–	–	80	–	–	−4.2	−4.2	−5.0	81	97	71
Desipramine	266	10.16 (B)	3.79	−3.3	–	–	100	–	–	−3.8	−4.1	−4.5	99	98	98
Fluvastatine	411	4.31 (A)[a]	4.17	−3.6	–	–	100	100	100[g]	−3.2	−3.7	−3.7	100	100	100
Furosemide	331	3.52 (A)	2.56	−4.8[i]	–	−4.5	61	54	60	−4.4	−4.7	−5.1	72	59	61
Hydrochlorothiazide	298	–	−0.03	−5.4	–	−4.7	67	–	65	−4.2	−4.5	−5.0	83	81	73
Ketoprofen	254	3.98 (A)	3.16	−3.1	–	−4.0	100	–	100	−3.5	−4.0	−4.2	100	99	100
Metoprolol	267	9.56 (B)	1.95	−3.9	–	−4.5	95	–	–	−4.5	−4.3	−5.3	58	92	47
Naproxen	230	4.18 (A)	3.24	−3.1	–	−3.7[j]	99	–	92	−3.4	−3.9	−4.1	100	100	100
Piroxicam	331	5.07 (A)	1.98	−3.2	–	−4.1	100	–	–	−3.7	−4.2	−4.4	100	97	99
Propranolol	259	9.53 (B)	3.48	−3.5	−4.2	−4.3	90	100	99	−3.6	−4.0	−4.3	100	99	100
Ranitidine	314	8.31 (B)	1.28	−4.6	–	−4.7	50	100	63	−4.4	−4.4	−5.2	67	88	56
Terbutaline	225	8.67 (B)	−0.08	−4.5	–	−5.3[j]	62	78	60	−4.5	−4.2	−5.2	62	95	51

[a] Compound set from Obata et al. (2005).
[b] Data from Avdeef (2003) unless otherwise noted.
[c] A: acid (pK_a < 6.5), B: base (pK_a > 6.5).
[d] Data from Lennernas 2007.
[e] Data from Lipka et al. (1998).
[f] Data from Zakeri-Milani et al. (2007).
[g] Data from Chiou et al. (2000).
[h] Data from Chiou and Barve (1998) unless otherwise noted.
[i] Data from Knutson et al. (2008).
[j] Data from Fagerholm et al. (1996).

divided by the fold and villi expansion (30) and adjusted for the difference of the P_{eff}–Fa scaling factor (=$2/r_{GI} \times DF \times T_{si}$) (previous value = 1.39×10^4, present value = 2.86×10^4). The density of the tight junction was assumed to be similar for both in vivo and in vitro.

2.2.4. Calculation of effective diffusion coefficient

The diffusion coefficient of monomer drug (D_{mono}) at 37 °C was calculated based on the method of Avdeef et al. (2004), and was corrected for the difference of viscosity between 25 °C and 37 °C by multiplying 1.41.

$$D_{mono} = 10^{-4.113-0.4609\times\log_{10}(MW)} \times 1.41 \quad (15)$$

2.2.5. Acc

Acc was calculated from $P_{ivv,m,tot}$, D_{mono} and villi morphology according to Oliver et al. (1998).

2.2.6. UWL permeability

P_{ivxUWL} can be calculated from the UWL thickness (h_{ivxUWL}) and D_{mono}.

$$P_{ivxUWL} = \frac{D_{mono}}{h_{ivxUWL}} \quad (16)$$

The UWL thickness was set to 300 μm and 3000 μm for in vivo and the in vitro system, respectively.

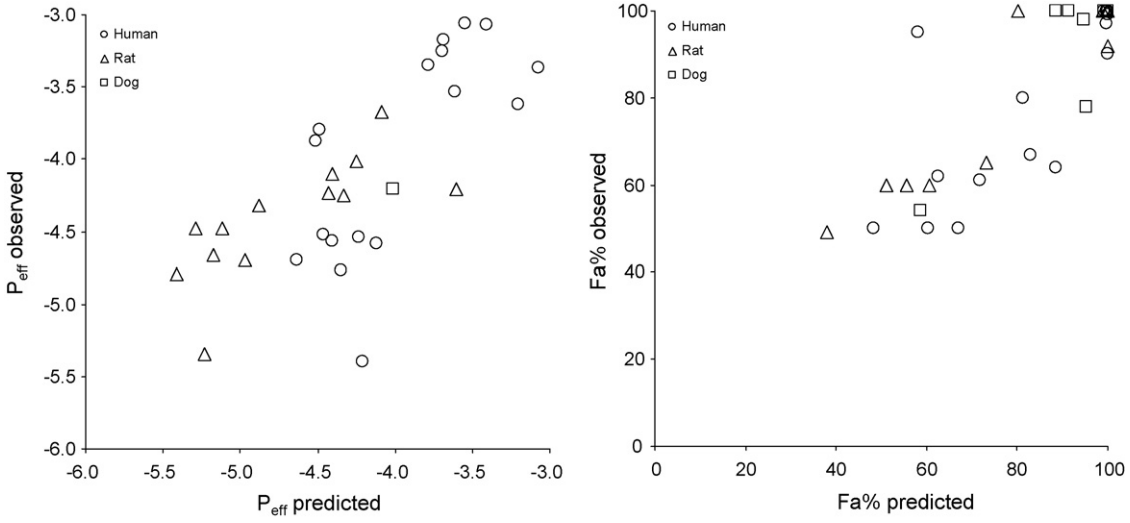

Fig. 1. P_{eff} and Fa% predictability of the theoretical scheme.

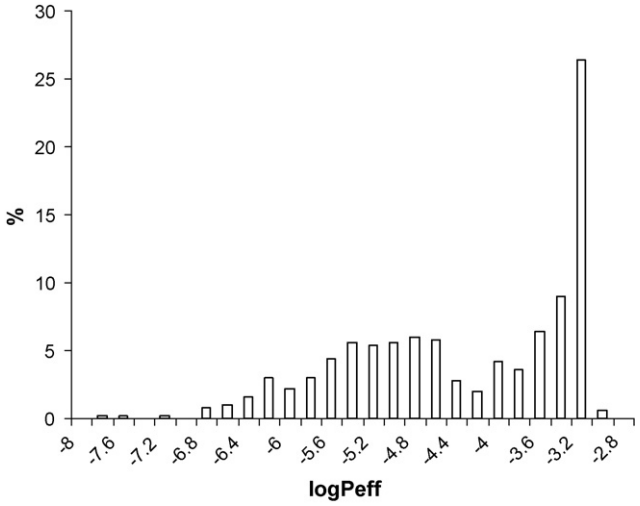

Fig. 2. Distribution of simulated human P_{eff} values at pH 6.5 for drug-like compounds.

2.3. Generation of virtual compounds by Monte Carlo method

Virtual compounds were generated by the Monte Carlo method, considering typical molecular properties of drug-like compounds (Wenlock et al., 2003). The normal distribution was assumed for $\log P_{oct}$ (2.5 ± 3 (mean $\pm$ S.D.) for acidic and basic compounds, 0.5 ± 3 for undissociable compounds), molecular weight (400 ± 100), and pK_a (4 ± 1 for acid, 8.5 ± 1 for base). The ratio of acidic: basic: undissociable compounds was set to be 20:60:20. Five hundred virtual compounds were generated. Two pH conditions for in vitro experiments were assumed, 6.5 and 7.4. For in vivo conditions, pH 6.0, 6.5 and 7.0 were used based on the observed variation of microclimate pH along the gastrointestinal tract (Said et al., 1986).

3. Results and discussion

P_{eff} estimation from in vitro data is one of the critical processes for successful oral absorption simulation. Therefore, the in vitro–in vivo extrapolation (IVIVE) should be investigated in detail. However, the number of available experimental human P_{eff} data is limited in the literature (Lennernaes, 2007). In addition, P_{eff} data often have large variation. Therefore, it was difficult to investigate IVIVE for structurally diverse compounds using experimental P_{eff} data. On the other hand, the theoretical calculation of the intestinal membrane permeation has been improved in recent years (Camenisch et al., 1996; Garmire and Hunt, 2008; Liu and Hunt, 2005; Obata et al., 2005; Sugano et al., 2006). In the present study, the Monte Carlo method was used to generate virtual compounds with drug-like physicochemical properties to calculate the virtual P_{eff}, $P_{ivt,app}$ and Fa% values.

The estimation scheme used in the present study was based on the theoretical passive absorption model (TPAM) previously reported (Obata et al., 2005; Sugano et al., 2006), replacing some lamp parameters with the GI structure parameters such as VE, FE and Acc. In addition, $P_{ivv,trans,0}$ was calculated from the relationship between the in vitro intrinsic permeability and $\log P_{oct}$, rather than using the parameter optimization process with clinical Fa% data as previously reported (Obata et al., 2005). Therefore, the estimation scheme used in the present study was further mechanistically reduced compared to the previous TPAM, enabling the theoretical investigation for in vitro–in vivo and species differences. The in vivo

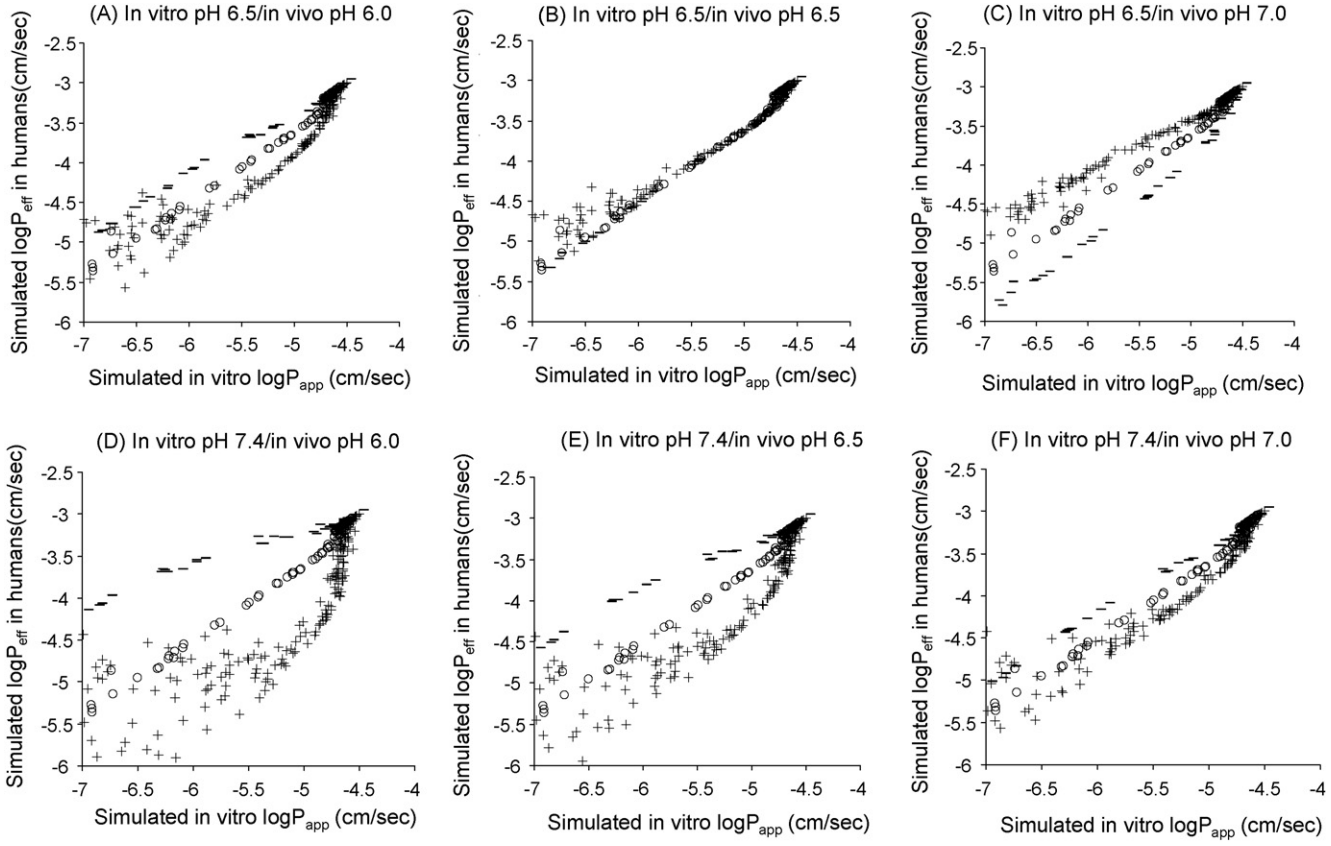

Fig. 3. Simulated human P_{eff} vs simulated $P_{ivt,app}$. In vitro pH /in vivo pH: (A) 6.5/6.0, (B) 6.5/6.5, (C) 6.5/7.0, (D) 7.4/6.0, (E) 7.4/6.5, (F) 7.4/7.0. The keys: acidic (−), basic (+), and neutral (○) compounds at physiological pH.

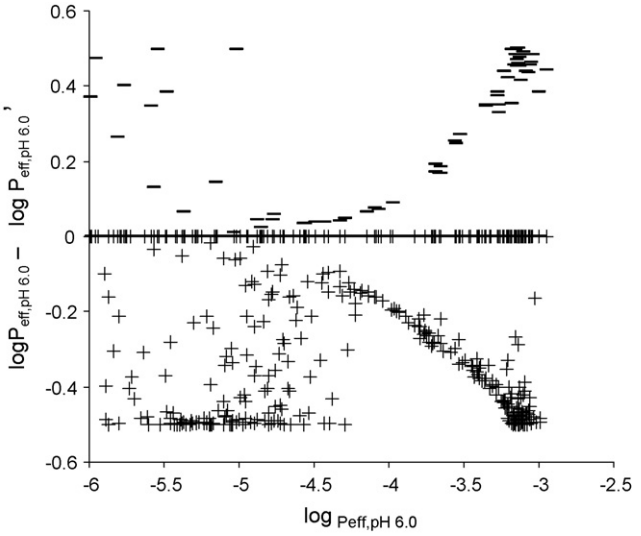

Fig. 4. The difference between the theoretical pH correction and overall pH correction on P_{eff}. The keys: acidic (−) and basic (+) compounds at physiological pH.

predictability of the present scheme was found to be similar with that reported for the previous TPAM (Table 1, Fig. 1).

The distribution of calculated P_{eff} values for drug-like compounds is shown in Fig. 2. Over 50% of the drug-like compounds were estimated to have $P_{eff} > 1.0 \times 10^{-4}$ cm/s which corresponds to Fa% > 80% (Lennernaes, 2007). This is in good agreement that drug likeness is related to favourable oral absorption. If $P_{eff} > 5 \times 10^{-4}$ cm/s, the UWL permeability dominates the P_{eff} value.

$P_{ivt,app}$–P_{eff} plot is shown in Fig. 3. When the same pH value was used for in vivo and in vitro, the scattering was small, whereas it was large when different pH values were used. Therefore, a simple linear regression cannot be used to estimate P_{eff} value from $P_{ivt,app}$ data when the pH of in vitro system is different from that of the in vivo intestine. The scatter of $P_{ivt,app}$–P_{eff} plot was more pronounced for basic compounds than for neutral and acidic compounds. Even when the same in vitro pH and in vivo pH values were used, the permeability of cationic compound may be underestimated by Caco-2 due to the difference of paracellular pathway (Fig. 3(B)).

The difference of UWL thickness had little effect on P_{app}–P_{eff} plot, because the expansion of surface area in vivo cancels out the thicker UWL in vitro. However, the effect of the UWL should be eliminated when structure permeability relationship is investigated (Fujikawa et al., 2007). In vitro UWL thickness depends on the agitation condition of the in vitro system (Youdim et al., 2003). Therefore, h_{ivtUWL} should be assessed for each in vitro system. The h_{ivtUWL} of a drug can be calculated from the pH permeability profile (Ruell et al., 2003). In addition, $R_{para,MW}$ and C for each in vitro system can be obtained by using paracellular pathway permeants with different molecular size and charge (Adson et al., 1994). If a control compound for paracellular permeation is added to each well, the difference of the paracellular pathway can be corrected, resulting in more accurate in vivo predictability for each test compound (Saitoh et al., 2004).

In a commercially available simulation programme, the P_{eff} value at pH 6.5 was directly corrected for the regional pH difference. When we apply pH partition theory directly for P_{eff} to correct the regional pH difference,

$$P'_{eff,pH} = P_{eff,pH6.5} \times \frac{f_{0,pH}}{f_{0,pH6.5}} \quad (17)$$

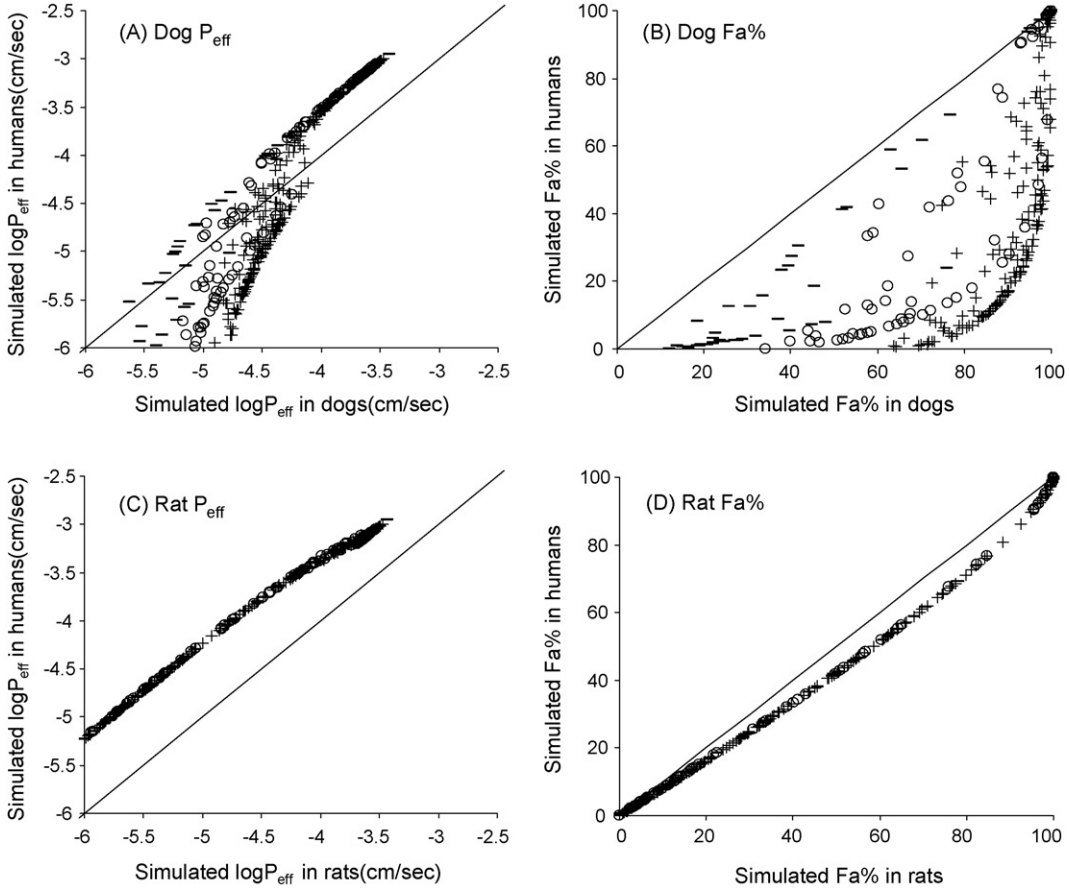

Fig. 5. Simulated species differences of P_{eff} and Fa%. The keys: acidic (−), basic (+), and neutral (○) compounds at physiological pH.

where additional subscript indicates pH (this equation is not the same as that in the software). The relationship between $P_{eff,pH6.0}$ and $P_{eff,pH6.0}-P'_{eff,pH6.0}$ is shown in Fig. 4. In the case of basic compounds, direct correction of P_{eff} resulted in under estimation at low and high P_{eff} region, whereas it resulted in over estimation in the case of acidic compounds. At low and high P_{eff} region, paracellular permeation and UWL permeation mainly determine P_{eff}, respectively. However, the pH partition theory is only applicable for transcellular permeation. Therefore, direct pH correction of P_{eff} resulted in the discrepancy between $P_{eff,pH6.0}$ and $P'_{eff,pH6.0}$.

Species difference was also investigated (Fig. 5). The paracellular pathway radius of dogs was set to be 1.5 times larger than that of humans, based on the molecular weight threshold value of PEG absorption (MW = ca. 400 for humans and rats, MW = ca. 600 for dogs) (He et al., 1998). It is well known that Fa% of dogs overestimates that of humans for paracellular pathway permeation (Chiou et al., 2000), whereas Fa% of rats is similar to that of humans (Chiou and Barve, 1998). The species difference of Fa% simulated in this study was in good agreement with the previous findings (Chiou and Barve, 1998; Chiou et al., 2000; He et al., 1998), suggesting that the theoretical calculation used in the present study was appropriate. The results of the present study suggested that P_{eff} value of dogs would be larger than that of humans for paracellular permeation, whereas smaller for transcellular and UWL limited permeation. The P_{eff} values of rats were smaller than that of humans for all compounds, reflecting the difference of small intestinal morphology. The species difference of P_{eff} simulated in this study was also in good agreement with the previous findings (Fagerholm et al., 1996; Lipka et al., 1998; Pappenheimer, 1998; Zakeri-Milani et al., 2007).

The scheme introduced in this study can be applied for theoretical P_{eff} estimation from in vitro data: (1) convert $P_{ivt,app}$ to $P_{ivt,trans,0}$ (Avdeef et al., 2005a), (2) convert $P_{ivt,trans,0}$ to $P_{ivv,trans}$ by the pH partition (A and B values in Eq. (9) should be obtained for each in vitro system), and (3) convert $P_{ivv,trans}$ to P_{eff} by adding paracellular pathway (Sugano et al., 2003, 2002), multiplying for villi expansion and villi surface accessibility (Oliver et al., 1998), adding UWL permeability, and multiplying for fold expansion.

In this study, the effect of bile micelles was not taken into account. In the case when a drug binds to bile micelles, UWL permeability becomes smaller due to the smaller diffusion coefficient of the bile micelle bound drug. In addition, epithelial membrane permeability also decreases due to the decrease of the free fraction. A calculation scheme to treat the effect of bile micelle binding was recently reported (Sugano, 2008).

In conclusion, for P_{eff} calculation from $P_{ivt,app}$, theoretical calculation was suggested to be more appropriate than simple empirical extrapolation by linear regression. In this study, a Monte Carlo method was applied to generate virtual drug-like compounds. This approach would be further applicable for investigating the effect of compound characteristics on in vivo and clinical biopharmaceutical profiles.

Acknowledgements

KS would like to thank Prof. Shinji Yamashita of Setsunan University for meaningful discussion. KS also would like to thank Mr. Michael Cram, Ms. Joanne Bennett and Dr. Mascha Van Den Berg for their kind supports.

References

Adson, A., Ruab, T.J., Burton, P.S., Barsuhn, C.L., Hilgers, A.R., Audus, K.L., Ho, N.F.H., 1994. Quantitative approaches to delineate paracellular diffusion in cultured epithelial cell monolayers. J. Pharm. Sci. 83, 1529–1530.

Atuma, C., Strugala, V., Allen, A., Holm, L., 2001. The adherent gastrointestinal mucus gel layer: thickness and physical state in vivo. Am. J. Physiol. 280, G922–G929.

Avdeef, A., 2003. Absorption and Drug Development. Wiley-Interscience.

Avdeef, A., Artursson, P., Neuhoff, S., Lazorova, L., Grasjo, J., Tavelin, S., 2005a. Caco-2 permeability of weakly basic drugs predicted with the Double-Sink PAMPA method. Eur. J. Pharm. Sci. 24, 333–349.

Avdeef, A., Artursson, P., Neuhoff, S., Lazorova, L., Grasjoe, J., Tavelin, S., 2005b. Caco-2 permeability of weakly basic drugs predicted with the Double-Sink PAMPA pKfluxa method. Eur. J. Pharm. Sci. 24, 333–349.

Avdeef, A., Nielsen, P.E., Tsinman, O., 2004. PAMPA—a drug absorption in vitro model: 11. Matching the in vivo unstirred water layer thickness by individual-well stirring in microtitre plates. Eur. J. Pharm. Sci. 22, 365–374.

Camenisch, G., Folkers, G., van de Waterbeemd, H., 1996. Review of theoretical passive drug absorption models: historical background, recent developments and limitations. Pharmaceutica Acta Helvetiae 71, 309–327.

Chiou, W.L., 1994. Effect of 'unstirred' water layer in the intestine on the rate and extent of absorption after oral administration. Biopharm. Drug Dispos. 15, 709–717.

Chiou, W.L., Barve, A., 1998. Linear correlation of the fraction of oral dose absorbed of 64 drugs between humans and rats. Pharm. Res. 15, 1792–1795.

Chiou, W.L., Jeong, H.Y., Chung, S.M., Wu, T.C., 2000. Evaluation of using dog as an animal model to study the fraction of oral dose absorbed of 43 drugs in humans. Pharm. Res. 17, 135–140.

DeSesso, J.M., Jacobson, C.F., 2001. Anatomical and physiological parameters affecting gastrointestinal absorption in humans and rats. Food Chem. Toxicol. 39, 209–228.

DeSesso, J.M., Williams, A.L., 2008. Contrasting the gastrointestinal tracts of mammals: Factors that influence absorption. Annu. Rep. Med. Chem. 43, 353–371.

Fagerholm, U., Johansson, M., Lennernaes, H., 1996. Comparison between permeability coefficients in rat and human jejunum. Pharm. Res. 13, 1336–1342.

Fagerholm, U., Lennernaes, H., 1995. Experimental estimation of the effective unstirred water layer thickness in the human jejunum, and its importance in oral drug absorption. Eur. J. Pharm. Sci. 3, 247–253.

Fujikawa, M., Nakao, K., Shimizu, R., Akamatsu, M., 2007. QSAR study on permeability of hydrophobic compounds with artificial membranes. Bioorg. Med. Chem. 15, 3756–3767.

Garmire, L.X., Hunt, C.A., 2008. In silico methods for unraveling the mechanistic complexities of intestinal absorption: metabolism-efflux transport interactions. Drug Metab. Dispos..

He, Y., Murby, S., Warhurst, G., Gifford, L., Walker, D., Ayrton, J., Eastmond, R., Rowland, M., 1998. Species differences in size discrimination in the paracellular pathway refrected by oral bioavailability of poly(ethylene glycol) and D-peptides. J. Pharm. Sci. 87, 626–633.

Kararli, T.T., 1995. Comparison of the gastrointestinal anatomy, physiology, and biochemistry of humans and commonly used laboratory animals. Biopharm. Drug Dispos. 16, 351–380.

Knipp, T.G., Ho, N.F.H., Barsuhn, C.L., Borchardt, R.T., 1997. Paracellular diffusion in Caco-2 cell monolayers: effect of perturbation on the transport of hydrophilic compounds that vary in size and charge. J. Pharm. Sci. 86, 1105–1110.

Knutson, T., Fridblom, P., Ahlstrom, H., Magnusson, A., Tannergren, C., Lennernas, H., 2008. Increased understanding of intestinal drug permeability determined by the LOC-I-GUT approach using multislice computed tomography. Mol. Pharm. 6, 2–10.

Lennernaes, H., 2007. Intestinal permeability and its relevance for absorption and elimination. Xenobiotica 37, 1015–1051.

Lipka, E., Spahn-Langguth, H., Mutschler, E., Amidon, G.L., 1998. In vivo non-linear intestinal permeability of celiprolol and propranolol in conscious dogs: evidence for intestinal secretion. Eur. J. Pharm. Sci. 6, 75–81.

Liu, Y., Hunt, C.A., 2005. Studies of intestinal drug transport using an in silico epithelio-mimetic device. BioSystems 82, 154–167.

Masaoka, Y., Tanaka, Y., Kataoka, M., Sakuma, S., Yamashita, S., 2006. Site of drug absorption after oral administration: assessment of membrane permeability and luminal concentration of drugs in each segment of gastrointestinal tract. Eur. J. Pharm. Sci. 29, 240–250.

Obata, K., Sugano, K., Saitoh, R., Higashida, A., Nabuchi, Y., Machida, M., Aso, Y., 2005. Prediction of oral drug absorption in humans by theoretical passive absorption model. Int. J. Pharm. 293, 183–192.

Oliver, R.E., Jones, A.F., Rowland, M., 1998. What surface of the intestinal epithelium is effectively available to permeating drugs? J. Pharm. Sci. 87, 634–639.

Pappenheimer, J.R., 1998. Scaling of dimensions of small intestines in non-ruminant eutherian mammals and its significance for absorptive mechanisms. Comp. Biochem. Physiol. A Mol. Integr. Physiol. 121, 45–58.

Parrott, N., Lave, T., 2008. Applications of physiologically based absorption models in drug discovery and development. Mol. Pharm. 5, 760–775.

Ruell, J.A., Tsinman, K.L., Avdeef, A., 2003. PAMPA—a drug absorption in vitro model*1: 5. Unstirred water layer in iso-pH mapping assays and pKaflux–optimized design (pOD-PAMPA). Eur. J. Pharm. Sci. 20, 393.

Said, H.M., Blair, J.A., Lucas, M.L., Hilburn, M.E., 1986. Intestinal surface acid microclimate in vitro and in vivo in the rat. J. Lab. Clin. Med. 107, 420–424.

Saitoh, R., Sugano, K., Takata, N., Tachibana, T., Higashida, A., Nabuchi, Y., Aso, Y., 2004. Correction of permeability with pore radius of tight junctions in Caco-2 monolayers improves the prediction of the dose fraction of hydrophilic drugs absorbed by humans. Pharm. Res. 21, 749.

Shirasaka, Y., Masaoka, Y., Kataoka, M., Sakuma, S., Yamashita, S., 2008. Scaling of in vitro membrane permeability to predict P-glycoprotein-mediated drug absorption in vivo. Drug Metab. Dispos. 36, 916–922.

Sugano, K., 2008. Estimation of effective intestinal membrane permeability considering bile micelle solubilisation. Int. J. Pharm., doi:10.1016/j.ijpharm.2008.10.001.

Sugano, K., Nabuchi, Y., Machida, M., Aso, Y., 2003. Prediction of human intestinal permeability using artificial membrane permeability. Int. J. Pharm. 257, 245–251.
Sugano, K., Obata, K., Saitoh, R., Higashida, A., Hamada, H., 2006. Processing of biopharmaceutical profiling data in drug discovery. In: Testa, B., Krämer, S., Wunderli-Allenspach, H., Folkers, G. (Eds.), Pharmacokinetic Profiling in Drug Research. Wiley-VCH, Zurich, pp. 441–458.
Sugano, K., Takata, N., Machida, M., Saitoh, K., Terada, K., 2002. Prediction of passive intestinal absorption using bio-mimetic artificial membrane permeation assay and the paracellular pathway model. Int. J. Pharm. 241, 241–251.
Sutton, S.C., 2004. Companion animal physiology and dosage form performance. Adv. Drug Deliv. Rev. 56, 1383–1398.
Tavelin, S., Taipalensuu, J., Hallboeoek, F., Vellonen, K.-S., Moore, V., Artursson, P., 2003. An Improved Cell Culture Model Based on 2/4/A1 Cell Monolayers for Studies of Intestinal Drug Transport: Characterization of Transport Routes. Pharm. Res. 20, 373–381.
van de Waterbeemd, H., Gifford, E., 2003. ADMET in silico modelling: towards prediction paradise? Nat. Rev. Drug Discov. 2, 192–204.
Wenlock, M.C., Austin, R.P., Barton, P., Davis, A.M., Leeson, P.D., 2003. A comparison of physiochemical property profiles of development and marketed oral drugs. J. Med. Chem. 46, 1250–1256.
Winne, D., 1978. The permeability coefficient of the wall of a villous membrane. J. Math. Biol. 6, 95–108.
Yamashita, S., Furubayashi, T., Kataoka, M., Sakane, T., Sezaki, H., Tokuda, H., 2000. Optimized conditions for prediction of intestinal drug permeability using Caco-2 cells. Eur. J. Pharm. Sci. 10, 195–204.
Youdim, K.A., Avdeef, A., Abbott, N.J., 2003. In vitro trans-monolayer permeability calculations: often forgotten assumptions. Drug Discov. Today 8, 997–1003.
Zakeri-Milani, P., Valizadeh, H., Tajerzadeh, H., Azarmi, Y., Islambolchilar, Z., Barzegar, S., Barzegar-Jalali, M., 2007. Predicting human intestinal permeability using single-pass intestinal perfusion in rat. J. Pharm. Pharm. Sci. 10, 368–379.